

# DeiSAM: Segment Anything with Deictic Prompting

Hikaru Shindo<sup>1</sup> Manuel Brack<sup>1,2</sup> Gopika Sudhakaran<sup>1,3</sup> Devendra Singh Dhami<sup>3,4</sup>  
Patrick Schramowski<sup>1,2,3,5</sup> Kristian Kersting<sup>1,2,3,6</sup>

## Abstract

Large-scale, pre-trained neural networks have demonstrated strong capabilities in various tasks, including zero-shot image segmentation. To identify concrete objects in complex scenes, humans instinctively rely on *deictic* descriptions in natural language, *i.e.*, referring to something depending on the context, such as “*The object that is on the desk and behind the cup.*”. However, deep learning approaches cannot reliably interpret such deictic representations as they have limited reasoning capabilities, particularly in complex scenarios. Therefore, we propose DeiSAM—a combination of large pre-trained neural networks with differentiable logic reasoners—for deictic promptable segmentation. Given a complex, textual segmentation description, DeiSAM leverages Large Language Models (LLMs) to generate first-order logic rules and performs differentiable forward reasoning on generated scene graphs. Subsequently, DeiSAM segments objects by matching them to the logically inferred image regions. As part of our evaluation, we propose the Deictic Visual Genome (DeiVG) dataset, containing paired visual input and complex, deictic textual prompts. Our empirical results demonstrate that DeiSAM is a substantial improvement over purely data-driven baselines for deictic promptable segmentation.

## 1. Introduction

Recently, large-scale neural networks have substantially advanced various tasks at the intersection of vision and language. One such challenge is grounded image segmentation, wherein objects within a scene are identified through textual descriptions. For instance, Grounding Dino (Liu et al., 2023b), combined with the Segment Anything Model

<sup>1</sup>Technical University of Darmstadt <sup>2</sup>German Research Center for AI (DFKI) <sup>3</sup>Hessian Center for AI (hessian.AI) <sup>4</sup>Eindhoven University of Technology <sup>5</sup>LAION <sup>6</sup>Centre for Cognitive Science, Technical University of Darmstadt . Correspondence to: Hikaru Shindo <hikaru.shindo@tu-darmstadt.de>.

Preprint.



“An object that is on the boat, and that is holding an umbrella”

Figure 1. DeiSAM segments objects with deictic prompting. Shown are segmentation masks with an input textual prompt. DeiSAM (ours, right) correctly segments the *people* on the boat holding umbrellas, whereas the neural baselines (left) incorrectly segment the *boat* instead. (Best viewed in color)

(SAM) (Kirillov et al., 2023), excels at this task if provided with appropriate prompts. However, a well-documented limitation of data-driven neural approaches is their lack of reasoning capabilities (Shi et al., 2023; Huang et al., 2023). Consequently, they often fail to understand complex prompts that require high-level reasoning on relations and attributes of multiple objects, as demonstrated in Fig. 1.

In contrast, humans identify objects through structured descriptions of complex scenes referring to an object depending on the context, *e.g.*, “*An object that is on the boat and holding an umbrella.*”. These descriptions are referred to as *deictic representations* and were introduced to artificial intelligence research motivated by linguistics (Agre & Chapman, 1987), and subsequently applied in reinforcement learning (Finney et al., 2002). Although deictic representations play a central role in human comprehension of scenes, current approaches fail to interpret them faithfully due to their poor reasoning capabilities.

To remedy these issues, we propose DeiSAM, which is a combination of large pre-trained neural networks with differentiable logic reasoners for deictic promptable object detection and segmentation. The DeiSAM pipeline is highly modular and fully differentiable, sophisticatedly integrating large pre-trained networks and neuro-symbolic reasoners. Specifically, we leverage Large Language Models (LLMs) to generate logic rules for a given deictic prompt

<sup>0</sup><https://github.com/IDEA-Research/Segment-Anything>

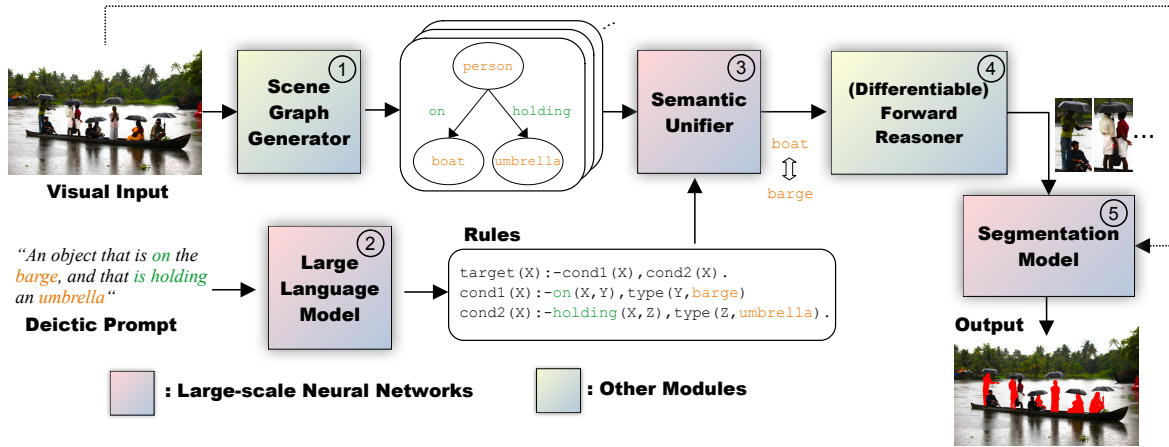


Figure 2. **DeiSAM architecture.** An image paired with a deictic prompt is given as input. We parse the image into a scene graph (1) and generate logic rules (2) corresponding to the deictic prompt using a large language model. The generated scene graph and rules are fed to the *Semantic Unifier* module (3), where synonymous terms are unified. For example, boat in the scene graph and barge in the generated rules will be interpreted as the same term. Next, the forward reasoner (4) infers target objects specified by the textual deictic prompt. Lastly, we perform object segmentation (5) on extracted cropped image regions of the target objects. Since the forward reasoner is differentiable (Shindo et al., 2023a), gradients can be passed through the entire pipeline. (Best viewed in color)

and perform differentiable forward reasoning (Shindo et al., 2023a;b) with scene graph generators (Zellers et al., 2018). The reasoner is efficiently combined with neural networks by leveraging forward propagation on computational graphs. The result of this reasoning step is used to ground a segmentation model that reliably identifies the objects best matching the input.

In summary, we make the following contributions: 1) We propose DeiSAM<sup>1</sup>, a modular, neuro-symbolic reasoning pipeline on LLMs and scene graphs for object segmentation with complex textual prompts. 2) We introduce a novel Deictic Visual Genome (DeiVG) benchmark that contains visual scenes paired with deictic representations, *i.e.*, complex textual identifications of objects in the scene. 3) We empirically demonstrate that DeiSAM strongly outperforms neural baselines for deictic segmentation. 4) We showcase that DeiSAM can perform end-to-end training via differentiable reasoning to improve the segmentation quality adapting to complex downstream reasoning tasks.

## 2. Related Work

**Multi-modal Large Language Models.** The recent achievements of large language models (LLMs) (Brown et al., 2020) have led to the development of multi-modal models, including vision-language models (Radford et al., 2021; Alayrac et al., 2022; Li et al., 2022a; Liu et al., 2023a), which take visual and textual inputs. However, these large models’ reasoning capabilities are limited (Huang et al., 2023), often

<sup>1</sup>Code: <https://github.com/ml-research/deictic-segment-anything>

inferring wrong conclusions when confronted with complex reasoning tasks. DeiSAM addresses these issues by combining large models with (differentiable) reasoners.

Additionally, DeiSAM is related to prior work using LLMs for program generation. For example, LLMs have been applied to generate probabilistic programs (Wong et al., 2023), Answer Set Programs (Ishay et al., 2023; Yang et al., 2023), and programs for visual reasoning (Surís et al., 2023; Stanić et al., 2024). These works have demonstrated that LLMs are powerful program generators and outperform simple zero-shot reasoning. With DeiSAM we propose the usage of LLMs to generate differentiable logic programs for image segmentation and object detection.

**Scene Graph Generation.** Scene Graph Generators (SGGs) encode complex visual relations to a summary graph using the comprehensive contextual knowledge of relation encoders (Lu et al., 2016; Zellers et al., 2018; Tang et al., 2019). Recently, the focus has shifted to transformer-based SGGs that use attention to capture global context while improving visual and semantic fusion (Dong et al., 2022; Lin et al., 2020; Lu et al., 2021). Lately, attention has also been used to capture object-level relation cues using visual and geometric features (Sudhakaran et al., 2023). The modularity of DeiSAM allows for using any SGG to obtain graph representations of input visual scenes.

**Visual Reasoning and Segmentation.** Visual Reasoning has been a fundamental problem in machine learning research, resulting in multiple benchmarks (Antol et al., 2015; Johnson et al., 2017; Yi et al., 2020) to address this topic and subsequent frameworks (Yi et al., 2018; Mao et al., 2019; Amizadeh et al., 2020; Hsu et al., 2023) that per-

form reasoning using symbolic programs and multi-modal transformers (Tan & Bansal, 2019). These benchmarks are primarily developed to answer queries written in natural language texts paired with visual inputs. Our proposed dataset, DeiVG, is the first to integrate complex textual prompts into the task of image segmentation with natural images. In a similar vein, to tackle visual reasoning tasks, neuro-symbolic rule learning frameworks have been proposed, where discrete rule structures are learned via backpropagation (Evans & Grefenstette, 2018; Minervini et al., 2020; Shindo et al., 2023a;b; Zimmer et al., 2023). These works have primarily been tested on visual arithmetic tasks and dedicated synthetic environments for reasoning (Stammer et al., 2021). DeiSAM is a unique neuro-symbolic framework that addresses image segmentation in natural images and utilizes differentiable reasoning for program learning.

Semantic segmentation aims to generate objects’ segmentation masks given visual input (Wang et al., 2018; Guo et al., 2018). Multiple datasets and tasks have been proposed that assess a model’s reasoning ability when identifying specific objects (Kazemzadeh et al., 2014; Yu et al., 2016). Recently, Segment Anything Model (SAM) (Kirillov et al., 2023) has been released, achieving strong results on zero-shot image segmentation tasks. Grounded SAM combines Grounding DINO (Liu et al., 2023b) with SAM, allowing for objects described by textual prompts. Moreover, LLMs have been utilized to perform multi-modal image segmentation (Lai et al., 2023), where the entire reasoning is conducted implicitly in a neural fashion. In contrast, DeiSAM integrates differentiable logic reasoners, encoding the reasoning process explicitly to avoid neural networks’ non-faithful behavior.

### 3. DeiSAM

Before discussing the DeiSAM pipeline, let us establish the necessary formal background of the framework.

**First-Order Logic and Differentiable Reasoning.** An *atom* is a formula  $p(t_1, \dots, t_n)$ , where  $p$  is a predicate symbol (e.g. `type`) and  $t_1, \dots, t_n$  are terms. A term is a variable or a constant. A *ground atom* or simply a *fact* is an atom with no variables (e.g. `type(obj1, boat)`). A *literal* is an atom ( $A$ ) or its negation ( $\neg A$ ), and a *clause* is a finite disjunction ( $\vee$ ) of literals. A *definite clause* is a clause with exactly one positive literal. If  $A, B_1, \dots, B_n$  are atoms, then  $A \vee \neg B_1 \vee \dots \vee \neg B_n$  is a definite clause. We write definite clauses in the form of  $A :- B_1, \dots, B_n$ , and refer to them as *rules* for simplicity in this paper. *Forward Reasoning* is a data-driven approach of reasoning in FOL (Russell & Norvig, 2010), i.e., given a set of facts and a set of rules, new facts are deduced by applying the rules to the facts. Differentiable forward reasoners compute logical entailment using tensor representations (Evans & Grefenstette, 2018; Shindo et al., 2023a) or graph neural



Figure 3. Examples from the Deictic Visual Genome (DeiVG) benchmark. Each entry consists of a deictic prompt of varying complexity (1-3 relations) and a image with annotations of objects corresponding to the prompt. For each complexity level we provide a set of 10k prompts, with images and annotations.

networks (Shindo et al., 2023b), and perform rule learning using gradients given labeled examples in the form of inductive logic programming (Cropper & Dumancic, 2022).

#### 3.1. Deictic Segmentation

Let us now devise the DeiSAM pipeline by giving a brief overview of its modules before describing essential components in more detail. Fig. 2 shows a schematic overview of the proposed workflow.

First, an input image is transferred into a graphical representation using a **(1) Scene Graph Generator**. Specifically, a scene graph comprises a set of triplets  $(n_1, e, n_2)$ , where entities  $n_1$  and  $n_2$  have relation  $e$ . For example, a *person* ( $n_1$ ) is *holding* ( $e$ ) an *umbrella* ( $n_2$ ). Consequently, each triplet can be interpreted as a fact,  $e(n_1, n_2)$ . The textual deictic prompt needs to be interpreted as a structured logical expression to perform reasoning on these facts. For this step, DeiSAM leverages **(2) Large Language Models**, which can generate logic rules for deictic descriptions, given sufficiently restrictive prompts as we demonstrate. In our example, the LLM would translate “An object that is on the barge, and that is holding an umbrella” into

```
cond1(X) :- on(X, Y), type(Y, barge).
cond2(X) :- holding(X, Y), type(Y, umbrella).
target(X) :- cond1(X), cond2(X).
```

where the first two rules define the conditions described in the prompt, and the last rule identifies corresponding objects. However, users often use terminology different from that of the SGG, e.g., *barge* and *boat* target the same concept but will not be trivially matched. To bridge the semantic gap, we introduce a **(3) semantic unifier**. This module leverages word embeddings of labels, entities, and relations in the generated scene graphs and rules to match synonymous terms by modifying rules accordingly. The semantically unified rules are then compiled to a **(4) forward reasoner**, which computes logical entailment using forward chaining (Shindo et al., 2023a). The reasoner identifies the targeted objects and their bounding boxes from the scene graph. Lastly, we segment the object by feeding the cropped images to a **(5) segmentation model**.

Now, let us investigate the two core modules of DeiSAM in detail: generating logic rules and reasoning.

### 3.1.1. LLMs AS LOGIC GENERATORS

To perform reasoning on textual prompts, we need to identify corresponding rules. We use LLMs to parse textual descriptions to logic rules using the following system prompt:

```
Given a deictic representation and available
predicates, generate rules in the format.
target(X):-cond1(X),...condn(X).
cond1(X):-pred1(X,Y),type(Y,const1).
...
condn(X):-predn(X,Y),type(Y,const2).
Use predicates and constants that appear in the
given sentence.
Capitalize variables: X, Y, Z, W, etc.
```

DeiSAM uses a specific rule format describing object and attribute relations. For example, a fact `on(person,boat)` in a scene graph would be decomposed into multiple facts `on(X,Y)`, `type(X,person)`, and `type(Y,boat)` to account for several entities with the same attribute in the scene.

The computational and memory cost of forward reasoning is determined by the number of variables over all rules and the number of conditions. Naive formatting of rules (Shindo et al., 2023b) leads to an exponential resource increase with the growing complexity of deictic prompts. Since the representations used in the forward reasoner are pre-computed and kept in memory, non-optimized approaches will quickly lead to exhaustive memory consumption (Evans & Grefenstette, 2018). In our format, however, we restrict the used variables to X and Y and only increase the number of rules with growing prompt complexity. Thus resulting in *linear* scaling of computational costs instead.

### 3.1.2. REASONING WITH DEICTIC PROMPTING

DeiSAM performs differentiable forward reasoning as follows. We build a reasoning function  $f_{reason} : \mathcal{G} \times \mathcal{R} \rightarrow \mathcal{T}$  where  $\mathcal{G}$  is a set of facts that represent a scene graph,  $\mathcal{R}$  is a set of rules generated by an LLM, and  $\mathcal{T}$  is a set of facts that represent identified target objects in the scene.

**(Differentiable) Forward Reasoning.** For a visual input  $x \in \mathbb{R}^2$ , DeiSAM utilizes scene graph generators (Gu et al., 2019) to obtain a logical graph representation  $\mathcal{G}$ , where each fact `rel(obj1,obj2)`  $\in \mathcal{G}$  represents an edge in the scene graph. Each fact in a given set  $\mathcal{G}$  is mapped to a confidence score using a *valuation vector*  $v \in [0, 1]^{|\mathcal{G}|}$ . A SGG is a function  $sgg : \mathbb{R}^2 \rightarrow [0, 1]^{|\mathcal{G}|}$  that produces a valuation vector out of a visual input. DeiSAM builds on the neuro-symbolic message-passing reasoner (NEUMANN) (Shindo et al., 2023b) to perform reasoning. For a given set of rules  $\mathcal{R}$ , DeiSAM constructs a *forward reasoning graph*, which is a bi-directional graph representation of a logic program. Given an initial valuation vector produced by an SGG,

DeiSAM computes logical consequences in a differentiable manner by performing bi-directional message passing on the constructed reasoning graph using soft-logic operations (See App. A for more details). DeiSAM identifies target objects to be segmented using confidence scores over facts representing targets, e.g., `target(obj1)`, and extracts the corresponding bounding boxes from the scene graph.

**Semantic Unifier.** DeiSAM unifies diverging semantics in the generated rules and scene graph using concept embeddings similar to neural theorem provers (Rocktäschel & Riedel, 2017). We rewrite the corresponding rules  $\mathcal{R}$  of a prompt by identifying the most similar terms in the scene graph for each predicate and constant. If rule  $R \in \mathcal{R}$  contains a term  $x$ , which does not appear in scene graph  $\mathcal{G}$ , we compute the most similar term as  $\arg \max_{y \in \mathcal{G}} \text{encoder}(x)^\top \cdot \text{encoder}(y)$ , where *encoder* is an embedding model for texts. We apply this procedure to terms and predicates individually.

## 4. Deictic Visual Genome

To facilitate a thorough evaluation of the novel deictic object segmentation tasks, we introduce the Deictic Visual Genome (DeiVG) dataset. Building on Visual Genome (Krishna et al., 2017), we construct pairs of deictic prompts and corresponding object annotations for real-world images. Our analysis of the scene graphs in Visual Genome found the annotations to often be noisy and ambiguous, which aligns with observations from previous research (Hudson & Manning, 2019). Consequently, we substantially filtered and cleaned potential candidates to produce a sound dataset.

First, we restricted ourselves to 19 commonly occurring relations and subsequently ensured that prompts were unambiguous, with only one kind of target object satisfying the prompt. Specifically, DeiVG contains prompts requiring the correct identification and segmentation of multiple objects, but these are guaranteed to be the same type according to Visual Genomes synset annotations. We automatically synthesize prompts from the filtered scene graphs using textual templates and NLP. e.g., the relations `on(cable,table)` and `behind(cable,mug)`, would yield a prompt "An object that is on the table and that is behind the mug" targeting the cable. Entries in the DeiVG dataset can be categorized by the number of relations they use in their object description. We introduce three subsets with 1-3 relations, which we denote as DeiVG<sub>1</sub>, DeiVG<sub>2</sub>, and DeiVG<sub>3</sub>, respectively. For each set, we randomly select 10k samples that we make available to the community to encourage further research.

## 5. Experiments

With the methodology of DeiSAM and our novel evaluation benchmark DeiVG, we now provide empirical and quali-

Method	Mean Average Precision (%) $\uparrow$		
	DeiVG <sub>1</sub>	DeiVG <sub>2</sub>	DeiVG <sub>3</sub>
SEEM	1.58	4.44	7.54
OFA-SAM	3.37	9.01	15.38
GLIP-SAM	2.32	0.03	0.00
GroundedDino-SAM	10.48	32.33	46.04
DeiSAM (ours)	<b>65.14</b>	<b>85.40</b>	<b>87.83</b>

Table 1. **DeiSAM handles deictic prompting.** Mean Average Precision (mAP) of DeiSAM and neural baselines on DeiVG datasets are shown. Subscript numbers indicate the complexity (hops on scene graph) of prompts.

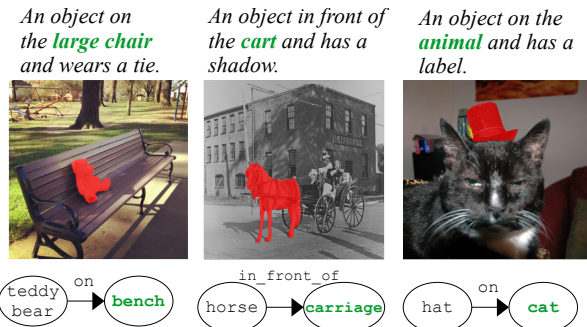


Figure 4. **DeiSAM can reason on ambiguous prompts.** Segmentation results (middle) on prompts (top) that contain entities not appearing in the scene graphs (bottom). DeiSAM successfully identified synonymous objects. (Best viewed in color)

tative experiments. Our results outline DeiSAM’s benefits over purely neural approaches and investigate the impact of individual DeiSAM components in more detail.

### 5.1. Experimental Setup

We base our experiments on the three subsets of DeiVG. As evaluation metric, we use mean average precision (mAP) over object classes. Since the object segmentation quality largely depends on the used segmentation model, we focus on assessing the object identification preceding the segmentation step. The default DeiSAM configuration for the subsequent experiments uses the ground truth scene graphs from Visual Genome (Krishna et al., 2017), gpt-3.5-turbo<sup>2</sup> as LLM for rule generation, ada-002<sup>3</sup> as embedding model for semantic unification, and SAM (Kirillov et al., 2023) for object segmentation. Additionally, we provide few-shot examples of deictic prompts and paired rules in the input context of the LLM, which improves performance (See App. C for detail). We present detailed ablations on each component of the DeiSAM pipeline in Sec. 5.4. We compare DeiSAM to multiple purely neural approaches, both empirically as well as qualitatively. We include three baselines that use one model for object identification and subsequently segment the grounded image using SAM (Kirillov et al.,

<sup>2</sup><https://openai.com/blog/introducing-chatgpt-and-whisper-apis>

<sup>3</sup><https://openai.com/blog/new-and-improved-embedding-model>

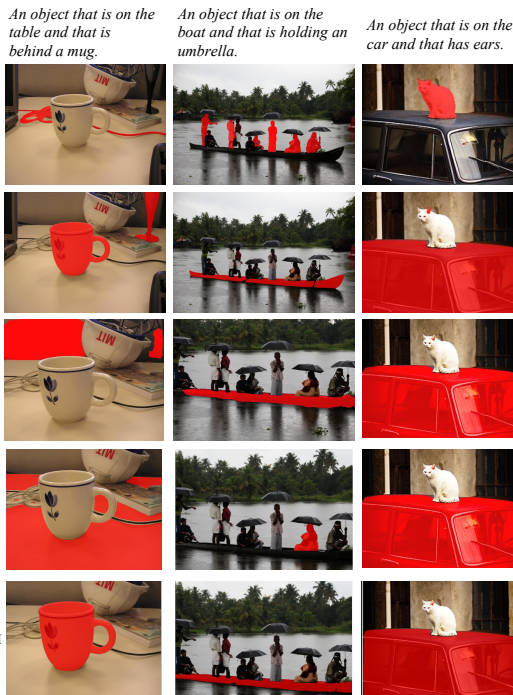


Figure 5. **DeiSAM segments objects with deictic prompts.** Segmentation results on the DeiVG dataset using DeiSAM and baselines are shown with deictic prompts on the top. DeiSAM correctly identifies and segments objects given deictic prompts (top row), while the baselines often segment a wrong object or fail to identify an object (bottom rows). More results are available in Fig. 11 in the Appendix. (Best viewed in color)

2023), similar to the grounding performed by DeiSAM. In our comparison, we include the following models for visual grounding: 1) One-For-All (OFA) (Wang et al., 2022), a unified transformer-based sequence-to-sequence model for vision and language tasks of which we use a dedicated visual grounding checkpoint<sup>4</sup>. 2) Grounded Language-Image Pre-training (GLIP) (Li et al., 2022b) a model for specifically designed for object-aware and semantically-rich object detection and grounding. 3) GroundingDino (Liu et al., 2023b) an open-set object detector combining transformer-based detection with grounded pre-training. Lastly, we compare to an end-to-end semantic segmentation model supporting textual prompts with SEEM (Zou et al., 2023).

### 5.2. Empirical Evidence

The results on DeiVG of all baselines compared to DeiSAM are summarized in Tab. 1. DeiSAM clearly outperforms all purely neural approaches by a large margin on all three splits of DeiVG. The performance of most methods improves with more descriptive deictic prompts, *i.e.*, more

<sup>4</sup>[https://modelscope.cn/models/damo/ofa\\_visual-grounding\\_refcoco\\_large\\_en/summary](https://modelscope.cn/models/damo/ofa_visual-grounding_refcoco_large_en/summary)

relations being used. We attribute this effect to two distinct causes. On the one hand, additional information describing the target object contributes to higher accuracy in object detection. On the other hand, DeiVG<sub>1</sub> contains significantly more samples with multiple target objects than DeiVG<sub>2</sub> or DeiVG<sub>3</sub>. Consequently, cases in which a method identifies only one out of multiple objects will have a higher impact on the overall performance. Overall, the large gap between DeiSAM and all baselines highlights the lack of complex reasoning capabilities in prevalent models and DeiSAM’s large advantage.

### 5.3. Qualitative Evaluation

After empirically demonstrating DeiSAM’s capabilities, we look into some qualitative examples. In Fig. 4, we demonstrate the efficacy of the semantic unifier. All examples use terminology in the deictic prompt diverging from the scene graph entity names. Nonetheless, the unification step successfully maps synonymous terms and still produces the correct segmentation masks, overcoming the limitation of off-the-shelf symbolic logic reasoners.

In Fig. 5, we further compare DeiSAM with the purely neural baselines. DeiSAM produces the correct segmentation mask even for complicated shapes (*e.g.*, partially occluded cable) or complex scenarios (*e.g.*, multiple people, only some holding umbrellas). All baseline methods, however, regularly fail to identify the correct object. A common failure mode is confounding nouns in the deictic prompt. For example, when describing an object in relation to a ‘boat’, the boat itself is identified instead of the target object. These examples strongly illustrate the improvements of DeiSAM over the pure neural approach on reasoning tasks.

### 5.4. Ablations

The modular nature of the DeiSAM pipeline enables easy variations of its components. Subsequently, we investigate the performance of key modules in isolation and their overall influence on the entire pipeline.

**LLM Rule Generation.** One of the key steps for DeiSAM is the translation of deictic prompts posed in natural language into syntactically and semantically sound logic rules. We observed that the performance of instruction-tuned LLMs on this task heavily depends on the employed prompting technique. Consequently, we leverage the well-known methods of few-shot prompting (Brown et al., 2020) and problem decomposition through chain-of-thought (CoT) (Wei et al., 2022). To that end, we first let the model extract all predicates from a deictic prompt, which we subsequently provide as additional context for the rule generation. For both cases, we provide multiple few-shot examples of varying complexity. We evaluate all prompting approaches with Llama-2-13B (Touvron et al., 2023) in Tab. 2. It shows that

Prompting Technique	Overall Success (%) ↑		
	DeiVG <sub>1</sub>	DeiVG <sub>2</sub>	DeiVG <sub>3</sub>
Instruct Only	0.00	0.00	0.00
CoT	0.00	0.00	0.00
Few-shot	<b>94.04</b>	92.52	90.17
Few-shot + CoT	91.00	<b>95.17</b>	<b>93.45</b>

Table 2. Ablations on prompting techniques for rule generation w/ Llama-2-13B-Chat. Few-shot examples are imperative for rule generation with chain-of-thought (CoT) prompting providing additional improvements for complex deictic prompts.

few-shot examples are imperative to perform rule generation successfully. Additionally, CoT for predicate decomposition further improves the rule generation for complex prompts.

With the best prompting technique identified, we evaluated multiple open and closed-source language models of different sizes (cf. App. C.1). In general, all instruction-tuned models can generate logical rules from deictic prompts. However, larger models strongly outperform smaller ones, especially for more complex inputs. The overall best-performing model was gpt-3.5-turbo producing correct rules for DeiVG for 93.65% of all samples.

**Semantic Unification.** Next, we take a more detailed look into the semantic unification module of the DeiSAM pipeline. At this step, we bridge the semantic gap between differing formulations in the deictic prompt and the scene graph generator. To realistically evaluate this task, we created an exemplary benchmark based on synonyms in the visual genome. For roughly 2.5k scenes, we considered all objects in the scene graph and identified one object name that differed from its synset entry. Based on that synonym, the task is to identify the one, unique, synonymous object in the scene. For example, in an image containing a ‘table’, ‘couch’, ‘chair’, and ‘cupboard’ the query ‘sofa’ should identify the ‘couch’ as most likely synonym. Overall, the task is considerably more challenging than it may appear at first glance, with the best model only achieving a success rate of 72% (cf. App C.1). A common issue is cases where a semantically related object is considered more similar than the actual synonym. For example, the query ‘sofa’ is matched with ‘pillow’ instead of the targeted ‘couch’ or ‘trousers’ with ‘jacket’ instead of ‘pants’. These results motivate further research into the semantic unification process.

**Scene Graph Generator.** Lastly, we investigated the scene graph generator module, going beyond the ground truth scene graphs of Visual Genome. One of the key challenges in using a pre-trained SGG is the potential mismatch between the set of objects and annotations in DeiVG and the training data of the SGG. While we built on the latest version of Visual Genome with extended annotations (VG<sub>v1.4</sub>), an older version (Krishna et al., 2017) has been commonly used for benchmarking different SGGs by excluding non-

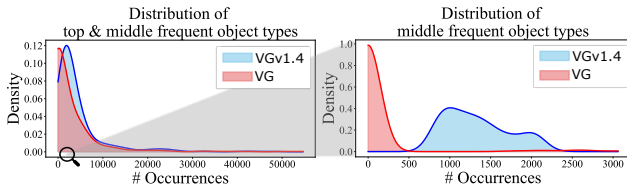


**Figure 6. The large discrepancy between DeiVG and standard Visual Genome.** DeiVG uses Visual Genome with extended annotations ( $VG_{v1.4}$ ), but the older version (VG) (Krishna et al., 2017) has been commonly used for SGG training. Object types are sorted w.r.t. the number of occurrences (x-axis) and their corresponding occupancies are shown (y-axis). The left plot is for top-and-middle frequent object types (0-50k #occ.), and the right plot is for middle frequent object types (0-3k #occ.).  $VG_{v1.4}$  contains many object types that do not appear in VG. (Best viewed in color)

frequent object types and relations (Xu et al., 2017). This preprocessed older version (VG) is still considered the standard benchmark for SGGs, which lacks many crucial objects and attributes in DeiVG built upon  $VG_{v1.4}$ .

We illustrate the discrepancy in Fig. 6, where we compare the Kernel Density Estimate (KDE) of  $VG_{v1.4}$  and VG. It shows that the newer version contains more types of objects in the top-and-middle frequency range. Additionally, many object types of  $VG_{v1.4}$  in the middle-frequency range are not contained at all in VG. Consequently, when parsing scenes from DeiVG with SGGs pre-trained on VG, the objects in the deictic prompt may not be contained in the generated scene graph at all. For example, for a given deictic prompt “an object that is wearing a black shirt”, we observed that the pre-trained SGG failed to detect *black shirt* because it was not included in its training data. This discrepancy leads to sub-par performance of DeiSAM with a pre-trained SGG, as shown in Tab. 3. While training the SGG specifically on the relevant scene distribution can partially address this issue, it is crucial to highlight that DeiSAM can be leveraged to improve SGGs as well. Our subsequent demonstration in Section 5.5 provides a glimpse of DeiSAM’s capabilities, showcasing its differentiable forward reasoner’s ability to perform end-to-end training, thereby unlocking new horizons in scene understanding and reasoning.

### 5.5. End-to-End Training of DeiSAM

Since DeiSAM employs a differentiable forward reasoner, a meaningful gradient signal can be back-propagated through the entire pipeline. Consequently, DeiSAM enables end-to-end learning on complex object detection and segmentation tasks with logical reasoning explicitly modeled during training. To illustrate this property, we show that DeiSAM can learn weighted mixtures of scene graph generators by propagating gradients through the reasoning module.

**Task.** Given SGGs  $sgg_1, sgg_2, \dots, sgg_n$ , we compose a

Method	Mean Average Precision (%) $\uparrow$	
	DeiVG <sub>1</sub>	DeiVG <sub>1</sub>
DeiSAM-VETO	6.64	15.92
DeiSAM-Mixture (naive)	37.61	59.81
DeiSAM-Mixture*	<b>64.44</b>	<b>86.57</b>

**Table 3. End-to-end training improves DeiSAM.** Mean Average Precision on the test split of the task of learning SGGs. DeiSAM-VETO uses a trained VETO model (Sudhakaran et al., 2023), DeiSAM-Mixture (naive) uses a mixture of a trained VETO model and VG scene graphs with randomly initialized weights, DeiSAM-Mixture\* uses the resulted mixture model after the weight optimization. DeiSAM improved the segmentation by learning parameters in the program by backpropagation.

DeiSAM model with a mixture of them, *i.e.*  $sgg(\mathbf{x}) = \sum_i w_i sgg_i(\mathbf{x})$  with  $w_i \in [0, 1]$  and  $sgg_i : \mathbb{R}^2 \rightarrow [0, 1]^{|\mathcal{G}|}$ , where  $\mathcal{G}$  is a set of facts to describe scene graphs. For example, the following program represents the mixture of scene graph generators for the deictic prompt “An object that has hair and that is on a surfboard”:

```
targetSgg(X, SG) :- cond1(X, SG), cond2(X, SG).
cond1(X, SG) :- hasSgg(X, Y, SG), typeSgg(Y, hair, SG).
cond2(X, SG) :- onSgg(X, Y, SG), onSgg(Y, surfboard, SG).
w_1: target(X) :- targetSgg(X, sgg1).
w_2: target(X) :- targetSgg(X, sgg2).
```

In contrast to Program 1, the program utilizes different SGGs and merges the results using learnable weights. The learning task is the optimization of weights  $w_i$  for downstream deictic segmentation. The differentiable reasoning pipeline in DeiSAM allows efficient gradient-based optimizations with automatic differentiation.

**Method.** Let  $(\mathbf{x}, p) \in \mathcal{D}$  be a DeiVG dataset, where  $\mathbf{x}$  is an input image, and  $p$  is a deictic prompt. For each input, DeiSAM produces segmentation masks  $\mathbf{M}_i$  with corresponding confidence score  $s_i$ , *i.e.*,  $\{(\mathbf{M}_i, s_i)\}_{i=0, \dots, n} = f_{deisam}(\mathbf{x}, p)$ . For each mask  $\mathbf{M}_i$ , we consider a binary label  $y_i \in \{0, 1\}$  using its corresponding bounding box and comparing with ground-truth masks with the IoU score, which assesses the quality of bounding boxes. For each instance  $(\mathbf{x}, p) \sim \mathcal{D}$ , we compute the binary-cross entropy loss:  $\ell = -\sum_{(\mathbf{M}_i, s_i) \sim f_{deisam}(\mathbf{x}, p)} (y_i \log s_i + (1 - y_i) \log(1 - s_i))$ . We minimize the loss  $\ell$  through gradient descent with respect to the rule weights in the differentiable programs.

**Experimental Setup.** We used VETO (Sudhakaran et al., 2023), which outperforms other SGGs on biased datasets where only some relations appear frequently. As the second ‘SGG’ for our weighted mixture model, we relied on ground-truth scene graphs from Visual Genome. We consider the following baselines: DeiSAM-VETO that only uses a pre-trained VETO model (Sudhakaran et al., 2023), DeiSAM-Mixture (naive) that uses a mixture of VETO and VG scene graphs with randomly initialized weights, and DeiSAM-

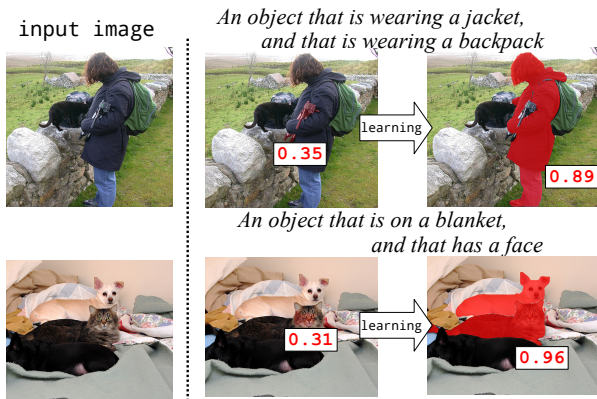


Figure 7. **DeiSAM can learn to produce better masks.** Shown are the input image (left) and target segmentation masks together with confidence scores obtained before (middle) and after (right) end-to-end training DeiSAM. DeiSAM improves the quality of segmentation by learning from examples. (Best viewed in color)

Mixture\* that uses the resulted mixture model after the weight optimization. We extracted instances from DeiVG datasets not used in VETO training (ca. 2000 samples), which we divided into a training, validation, and test split. We provide more experimental details in Sec. C.2.

**Result.** In Tab. 3, we compare the Mean Average Precision on the test split. The trained model DeiSAM-Mixture\* clearly outperforms the naive baseline, demonstrating successful training of the DeiSAM pipeline using gradients via differentiable reasoning. DeiSAM-VETO weak performance in the absence of ground-truth scene graphs can be attributed to objects that appear only on prompts but not its training data, as we discussed in Sec 5.4. Fig 7 shows examples of segmentation masks and their confidence scores produced by DeiSAM-Mixture models before and after training. Before learning, wrong or incomplete regions are segmented with low confidence scores because the reasoner fails to identify correct objects with low-quality scene graphs missing critical objects and relations. After learning, DeiSAM produces faithful segmentation masks and increased confidence scores. This highlights that DeiSAM improves the quality of scene graphs and the subsequent segmentation masks by learning using gradients, *i.e.*, it is a fully trainable pipeline with a strong capacity for complex logic reasoning.

## 6. Open Questions and Limitations

Our investigation of DeiSAM’s components highlights some clear avenues for future research. While LLMs perform well at parsing deictic prompts into logic rules with few-shot prompting, their performance could be improved further. For example, syntactically constrained sampling<sup>5</sup> or dedicated fine-tuning are promising approaches. Further, the

<sup>5</sup><https://github.com/IsaacRe/Syntactically-Constrained-Sampling>

Prompt: ‘An object that is wearing a helmet’

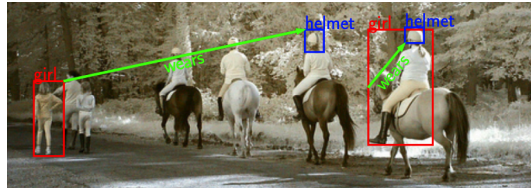


Figure 8. Example of erroneous annotations in Visual Genome leading to inconsistent examples in DeiVG. Here, the annotations for ‘helmet’ are incomplete and in one case, the relation ‘wears’ is linked to the wrong person. (Best viewed in color)

observed challenges in semantic unification could be addressed by specifically querying LLMs instead of using embedding models or providing multiple weighted unification candidates to the reasoner. Our results strongly support the intuitive assessment that generating rich scene graphs is key but difficult to achieve in a zero-shot fashion.

However, DeiSAM can play a vital role in improving scene graph generation. As we demonstrated, the differentiable pipeline can be utilized for meaningful training on complex downstream tasks. Thus allowing for the incorporation of real-world use cases in the training of SGGs in an end-to-end fashion. Further, DeiSAM can provide valuable information on general performance and failure cases of SGGs by investigating deictic segmentation tasks. Furthermore, the modularity of DeiSAM allows for easy integration of potential improvements to any of its components.

Upon manual inspection of the DeiVG dataset, we identified some inconsistent examples resulting from incomplete and erroneous scene graphs in Visual Genome that cannot be automatically cleaned up without external object identification. For example, the annotations shown in Fig. 8 lead to a DeiVG sample with two missing target objects and an incorrect one. We plan on building an even more consistent deictic segmentation benchmark using a cleanup process similar to GQA (Hudson & Manning, 2019).

## 7. Conclusion

We proposed DeiSAM to perform deictic object segmentation in complex scenes. DeiSAM effectively combines large-scale neural networks with differentiable forward reasoning in a modular pipeline. DeiSAM allows users to intuitively describe objects in complex scenes by their relations to other objects. Moreover, we introduced the novel Deictic Visual Genome (DeiVG) benchmark for segmentation with complex deictic prompts. In our extensive experiments, we demonstrated that DeiSAM strongly outperforms neural baselines highlighting its strong reasoning capabilities on visual scenes with complex textual prompts. To this end, our empirical results revealed open research questions and important future avenues of visual scene understanding.

## 8. Acknowledgements

This work was supported by the Federal Ministry of Education and Research (BMBF) AI lighthouse project “SPAICER” (01MK20015E), the EU ICT-48 Network of AI Research Excellence Center “TAILOR” (EU Horizon 2020, GA No 952215), and the Collaboration Lab “AI in Construction” (AICO). The work has also benefited from the Federal Ministry of Education and Research (BMBF) Competence Center for AI and Labour (“KompAKI”, FKZ 02L19C150) and from the Hessian Ministry of Higher Education, Research, Science and the Arts (HMWK) cluster projects “The Third Wave of AI” and “The Adaptive Mind”. We gratefully acknowledge support by the German Center for Artificial Intelligence (DFKI) project “SAINT”. It also benefited the HMWK / BMBF ATHENE project “AVSV”.

## References

- Agre, P. E. and Chapman, D. Pengi: An implementation of a theory of activity. In *Proceedings of the AAAI Conference on Artificial Intelligence (AAAI)*, 1987.
- Alayrac, J.-B., Donahue, J., Luc, P., Miech, A., Barr, I., Hasson, Y., Lenc, K., Mensch, A., Millican, K., Reynolds, M., Ring, R., Rutherford, E., Cabi, S., Han, T., Gong, Z., Samangooei, S., Monteiro, M., Menick, J. L., Borgeaud, S., Brock, A., Nematzadeh, A., Sharifzadeh, S., Bińkowski, M. a., Barreira, R., Vinyals, O., Zisserman, A., and Simonyan, K. Flamingo: a visual language model for few-shot learning. In *Proceedings of the Advances in Neural Information Processing Systems: Annual Conference on Neural Information Processing Systems (NeurIPS)*, 2022.
- Amizadeh, S., Palangi, H., Polozov, A., Huang, Y., and Koishida, K. Neuro-symbolic visual reasoning: Disentangling “Visual” from “Reasoning”. In *Proceedings of the International Conference on Machine Learning (ICML)*, 2020.
- Antol, S., Agrawal, A., Lu, J., Mitchell, M., Batra, D., Zitnick, C. L., and Parikh, D. Vqa: Visual question answering. In *Proceedings of the IEEE/CVF International Conference on Computer Vision (ICCV)*, 2015.
- Brown, T. B., Mann, B., Ryder, N., Subbiah, M., Kaplan, J., Dhariwal, P., Neelakantan, A., Shyam, P., Sastry, G., Askell, A., Agarwal, S., Herbert-Voss, A., Krueger, G., Henighan, T., Child, R., Ramesh, A., Ziegler, D. M., Wu, J., Winter, C., Hesse, C., Chen, M., Sigler, E., Litwin, M., Gray, S., Chess, B., Clark, J., Berner, C., McCandlish, S., Radford, A., Sutskever, I., and Amodei, D. Language models are few-shot learners. In *Proceedings of the Advances in Neural Information Processing Systems: Annual Conference on Neural Information Processing Systems (NeurIPS)*, 2020.
- Cropper, A. and Dumancic, S. Inductive logic programming at 30: A new introduction. *Journal of Artificial Intelligence Research (JAIR)*, 2022.
- Dong, X., Gan, T., Song, X., Wu, J., Cheng, Y., and Nie, L. Stacked hybrid-attention and group collaborative learning for unbiased scene graph generation. In *Proceedings of the IEEE/CVF Conference on Computer Vision and Pattern Recognition (CVPR)*, 2022.
- Evans, R. and Grefenstette, E. Learning explanatory rules from noisy data. *Journal of Artificial Intelligence Research (JAIR)*, 2018.
- Finney, S., Gardiol, N., Kaelbling, L. P., and Oates, T. The thing that we tried didn’t work very well: Deictic representation in reinforcement learning. In *Proceedings of Conference on Uncertainty in Artificial Intelligence (UAI)*, 2002.
- Gu, J., Zhao, H., Lin, Z., Li, S., Cai, J., and Ling, M. Scene graph generation with external knowledge and image reconstruction. In *Proceedings of the IEEE/CVF Conference on Computer Vision and Pattern Recognition (CVPR)*, 2019.
- Guo, Y., Liu, Y., Georgiou, T., and Lew, M. S. A review of semantic segmentation using deep neural networks. *Int. J. Multim. Inf. Retr.*, 2018.
- Hsu, J., Mao, J., Tenenbaum, J. B., and Wu, J. What’s left? concept grounding with logic-enhanced foundation models. In *Proceedings of the Advances in Neural Information Processing Systems: Annual Conference on Neural Information Processing Systems (NeurIPS)*, 2023.
- Huang, J., Chen, X., Mishra, S., Zheng, H. S., Yu, A. W., Song, X., and Zhou, D. Large language models cannot self-correct reasoning yet. *arXiv Preprint:2310.01798*, 2023.
- Hudson, D. A. and Manning, C. D. GQA: A new dataset for real-world visual reasoning and compositional question answering. In *Proceedings of the IEEE/CVF Conference on Computer Vision and Pattern Recognition (CVPR)*, 2019.
- Ishay, A., Yang, Z., and Lee, J. Leveraging large language models to generate answer set programs. In *Proceedings of the International Conference on Principles of Knowledge Representation and Reasoning (KR)*, 2023.
- Johnson, J., Hariharan, B., van der Maaten, L., Fei-Fei, L., Zitnick, C. L., and Girshick, R. Clevr: A diagnostic dataset for compositional language and elementary visual

- reasoning. In *Proceedings of the IEEE/CVF Conference on Computer Vision and Pattern Recognition (CVPR)*, 2017.
- Kazemzadeh, S., Ordonez, V., Matten, M., and Berg, T. ReferItGame: Referring to objects in photographs of natural scenes. In *Proceedings of the Conference on Empirical Methods in Natural Language Processing (EMNLP)*, 2014.
- Kirillov, A., Mintun, E., Ravi, N., Mao, H., Rolland, C., Gustafson, L., Xiao, T., Whitehead, S., Berg, A. C., Lo, W.-Y., Dollár, P., and Girshick, R. Segment anything. In *Proceedings of the IEEE/CVF International Conference on Computer Vision (ICCV)*, 2023.
- Krishna, R., Zhu, Y., Groth, O., Johnson, J., Hata, K., Kravitz, J., Chen, S., Kalantidis, Y., Li, L.-J., Shamma, D. A., et al. Visual genome: Connecting language and vision using crowdsourced dense image annotations. *International Journal of Computer Vision*, 2017.
- Lai, X., Tian, Z., Chen, Y., Li, Y., Yuan, Y., Liu, S., and Jia, J. Lisa: Reasoning segmentation via large language model. *arXiv Preprint:2308.00692*, 2023.
- Li, J., Li, D., Xiong, C., and Hoi, S. Blip: Bootstrapping language-image pre-training for unified vision-language understanding and generation. In *Proceedings of the International Conference on Machine Learning (ICML)*, 2022a.
- Li, L. H., Zhang, P., Zhang, H., Yang, J., Li, C., Zhong, Y., Wang, L., Yuan, L., Zhang, L., Hwang, J., Chang, K., and Gao, J. Grounded language-image pre-training. In *Proceedings of the IEEE/CVF Conference on Computer Vision and Pattern Recognition (CVPR)*, 2022b.
- Lin, X., Ding, C., Zeng, J., and Tao, D. GPS-Net: Graph property sensing network for scene graph generation. In *Proceedings of the IEEE/CVF Conference on Computer Vision and Pattern Recognition (CVPR)*, 2020.
- Liu, H., Li, C., Wu, Q., and Lee, Y. J. Visual instruction tuning. *arXiv Preprint:2304.08485*, 2023a.
- Liu, S., Zeng, Z., Ren, T., Li, F., Zhang, H., Yang, J., Li, C., Yang, J., Su, H., Zhu, J., et al. Grounding dino: Marrying dino with grounded pre-training for open-set object detection. *arXiv Preprint:2303.05499*, 2023b.
- Lu, C., Krishna, R., Bernstein, M., and Fei-Fei, L. Visual relationship detection with language priors. In *Proceedings of the European Conference on Computer Vision (ECCV)*, 2016.
- Lu, Y., Rai, H., Chang, J., Knyazev, B., Yu, G., Shekhar, S., Taylor, G. W., and Volkovs, M. Context-aware scene graph generation with Seq2Seq transformers. In *Proceedings of the IEEE/CVF International Conference on Computer Vision (ICCV)*, 2021.
- Mao, J., Gan, C., Kohli, P., Tenenbaum, J. B., and Wu, J. The Neuro-Symbolic Concept Learner: Interpreting Scenes, Words, and Sentences From Natural Supervision. In *Proceedings of the International Conference on Learning Representations (ICLR)*, 2019.
- Minervini, P., Riedel, S., Stenatorp, P., Grefenstette, E., and Rocktäschel, T. Learning reasoning strategies in end-to-end differentiable proving. In *Proceedings of the International Conference on Machine Learning (ICML)*, 2020.
- Radford, A., Kim, J. W., Hallacy, C., Ramesh, A., Goh, G., Agarwal, S., Sastry, G., Askell, A., Mishkin, P., Clark, J., Krueger, G., and Sutskever, I. Learning transferable visual models from natural language supervision. *arXiv Preprint:2103.00020*, 2021.
- Rocktäschel, T. and Riedel, S. End-to-end differentiable proving. In *Proceedings of the Advances in Neural Information Processing Systems: Annual Conference on Neural Information Processing Systems (NeurIPS)*, 2017.
- Russell, S. and Norvig, P. *Artificial Intelligence: A Modern Approach*. Prentice Hall, 3 edition, 2010.
- Shi, F., Chen, X., Misra, K., Scales, N., Dohan, D., Chi, E. H., Schärli, N., and Zhou, D. Large language models can be easily distracted by irrelevant context. In *Proceedings of the International Conference on Machine Learning (ICML)*, 2023.
- Shindo, H., Pfanschilling, V., Dhama, D. S., and Kersting, K.  $\alpha$ ilp: thinking visual scenes as differentiable logic programs. *Machine Learning Journal (MLJ)*, 2023a.
- Shindo, H., Pfanschilling, V., Dhama, D. S., and Kersting, K. Learning differentiable logic programs for abstract visual reasoning. *arXiv Preprint:2307.00928*, 2023b.
- Stammer, W., Schramowski, P., and Kersting, K. Right for the right concept: Revising neuro-symbolic concepts by interacting with their explanations. In *Proceedings of the IEEE/CVF Conference on Computer Vision and Pattern Recognition (CVPR)*, 2021.
- Stanić, A., Caelles, S., and Tschannen, M. Towards truly zero-shot compositional visual reasoning with llms as programmers. *arXiv Preprint:2401.01974*, 2024.
- Sudhakaran, G., Dhama, D. S., Kersting, K., and Roth, S. Vision relation transformer for unbiased scene graph generation. In *Proceedings of the IEEE/CVF International Conference on Computer Vision (ICCV)*, 2023.

- Surís, D., Menon, S., and Vondrick, C. Vipergpt: Visual inference via python execution for reasoning. In *Proceedings of the IEEE/CVF International Conference on Computer Vision (ICCV)*, 2023.
- Tan, H. and Bansal, M. LXMERT: learning cross-modality encoder representations from transformers. In *Proceedings of the Conference on Empirical Methods in Natural Language Processing (EMNLP)*, 2019.
- Tang, K., Zhang, H., Wu, B., Luo, W., and Liu, W. Learning to compose dynamic tree structures for visual contexts. In *Proceedings of the IEEE/CVF Conference on Computer Vision and Pattern Recognition (CVPR)*, 2019.
- Touvron, H., Lavril, T., Izacard, G., Martinet, X., Lachaux, M., Lacroix, T., Rozière, B., Goyal, N., Hambro, E., Azhar, F., Rodriguez, A., Joulin, A., Grave, E., and Lample, G. Llama: Open and efficient foundation language models. *arXiv:2302.13971*, 2023.
- Wang, P., Chen, P., Yuan, Y., Liu, D., Huang, Z., Hou, X., and Cottrell, G. W. Understanding convolution for semantic segmentation. In *Proceedings of IEEE Winter Conference on Applications of Computer Vision (WACV)*, 2018.
- Wang, P., Yang, A., Men, R., Lin, J., Bai, S., Li, Z., Ma, J., Zhou, C., Zhou, J., and Yang, H. OFA: unifying architectures, tasks, and modalities through a simple sequence-to-sequence learning framework. In *Proceedings of the International Conference on Machine Learning (ICML)*, 2022.
- Wei, J., Wang, X., Schuurmans, D., Bosma, M., Ichter, B., Xia, F., Chi, E. H., Le, Q. V., and Zhou, D. Chain-of-thought prompting elicits reasoning in large language models. In *Proceedings of the Advances in Neural Information Processing Systems: Annual Conference on Neural Information Processing Systems (NeurIPS)*, 2022.
- Wong, L., Grand, G., Lew, A. K., Goodman, N. D., Mansinghka, V. K., Andreas, J., and Tenenbaum, J. B. From word models to world models: Translating from natural language to the probabilistic language of thought. *arXiv Preprint:2306.12672*, 2023.
- Xu, D., Zhu, Y., Choy, C. B., and Fei-Fei, L. Scene graph generation by iterative message passing. In *Proceedings of the IEEE conference on computer vision and pattern recognition*, pp. 5410–5419, 2017.
- Yang, Z., Ishay, A., and Lee, J. Coupling large language models with logic programming for robust and general reasoning from text. In *Findings of the Association for Computational Linguistics (ACL)*, 2023.
- Yi, K., Wu, J., Gan, C., Torralba, A., Kohli, P., and Tenenbaum, J. Neural-symbolic VQA: disentangling reasoning from vision and language understanding. In *Proceedings of the Advances in Neural Information Processing Systems: Annual Conference on Neural Information Processing Systems (NeurIPS)*, 2018.
- Yi, K., Gan, C., Li, Y., Kohli, P., Wu, J., Torralba, A., and Tenenbaum, J. B. Clevrer: Collision events for video representation and reasoning. In *Proceedings of the International Conference on Learning Representations (ICLR)*, 2020.
- Yu, L., Poirson, P., Yang, S., Berg, A. C., and Berg, T. L. Modeling context in referring expressions. In *Proceedings of the European Conference on Computer Vision (ECCV)*, 2016.
- Zellers, R., Yatskar, M., Thomson, S., and Choi, Y. Neural motifs: Scene graph parsing with global context. In *Proceedings of the IEEE/CVF Conference on Computer Vision and Pattern Recognition (CVPR)*, 2018.
- Zimmer, M., Feng, X., Glanois, C., JIANG, Z., Zhang, J., Weng, P., Li, D., HAO, J., and Liu, W. Differentiable logic machines. *Transactions on Machine Learning Research (TMLR)*, 2023.
- Zou, X., Yang, J., Zhang, H., Li, F., Li, L., Gao, J., and Lee, Y. J. Segment everything everywhere all at once. *arXiv Preprint:2304.06718*, 2023.

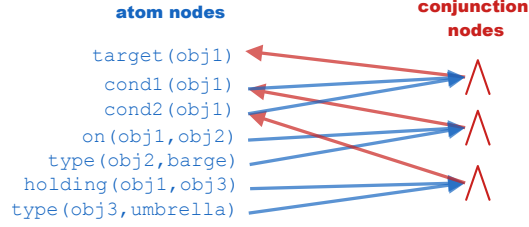


Figure 9. Forward reasoning graph for **Program 1**. A reasoning graph consists of *atom nodes* and *conjunction nodes*, and is obtained by grounding rules *i.e.*, removing variables by, *e.g.*,  $X \leftarrow \text{obj1}$ ,  $Y \leftarrow \text{obj2}$ . By performing bi-directional message passing on the reasoning graph using soft-logic operations, DeiSAM computes logical consequences in a differentiable manner. Only relevant nodes are shown. (Best viewed in color)

## A. Details of Forward Reasoning

DeiSAM employs a graph neural network-based differentiable forward reasoner (Shindo et al., 2023b), and we briefly explain the reasoning process. We represent a set of (weighted) rules as a directed bipartite graph. For example, Fig. 9 is a reasoning graph that represents **Program 1**.

**Definition A.1.** A *Forward Reasoning Graph* is a bipartite directed graph  $(\mathcal{V}_{\mathcal{G}}, \mathcal{V}_{\wedge}, \mathcal{E}_{\mathcal{G} \rightarrow \wedge}, \mathcal{E}_{\wedge \rightarrow \mathcal{G}})$ , where  $\mathcal{V}_{\mathcal{G}}$  is a set of nodes representing ground atoms (atom nodes),  $\mathcal{V}_{\wedge}$  is set of nodes representing conjunctions (conjunction nodes),  $\mathcal{E}_{\mathcal{G} \rightarrow \wedge}$  is set of edges from atom to conjunction nodes and  $\mathcal{E}_{\wedge \rightarrow \mathcal{G}}$  is a set of edges from conjunction to atom nodes.

DeiSAM performs forward-chaining reasoning by passing messages on the reasoning graph. Essentially, forward reasoning consists of *two* steps: (1) computing conjunctions of body atoms for each rule and (2) computing disjunctions for head atoms deduced by different rules. These two steps can be efficiently computed on bi-directional message-passing on the forward reasoning graph. We now describe each step in detail.

**(Direction  $\rightarrow$ ) From Atom to Conjunction.** First, messages are passed to the conjunction nodes from atom nodes. For conjunction node  $v_i \in \mathcal{V}_{\wedge}$ , the node features are updated:

$$v_i^{(t+1)} = \bigvee \left( v_i^{(t)}, \bigwedge_{j \in \mathcal{N}(i)} v_j^{(t)} \right), \quad (1)$$

where  $\bigwedge$  is a soft implementation of *conjunction*, and  $\bigvee$  is a soft implementation of *disjunction*. Intuitively, probabilistic truth values for bodies of all ground rules are computed softly by Eq. 1.

**(Direction  $\leftarrow$ ) From Conjunction to Atom.** Following the first message passing, the atom nodes are then updated using the messages from conjunction nodes. For atom node  $v_i \in \mathcal{V}_{\mathcal{G}}$ , the node features are updated:

$$v_i^{(t+1)} = \bigvee \left( v_i^{(t)}, \bigvee_{j \in \mathcal{N}(i)} w_{ji} \cdot v_j^{(t)} \right), \quad (2)$$

where  $w_{ji}$  is a weight of edge  $e_{j \rightarrow i}$ . We assume that each rule  $C_k \in \mathcal{C}$  has its weight  $\theta_k$ , and  $w_{ji} = \theta_k$  if edge  $e_{j \rightarrow i}$  on the reasoning graph is produced by rule  $C_k$ . Intuitively, in Eq. 2, new atoms are deduced by gathering values from different ground rules and from the previous step.

We used product for conjunction, and *log-sum-exp* function for disjunction:

$$\text{softor}^{\gamma}(x_1, \dots, x_n) = \gamma \log \sum_{1 \leq i \leq n} \exp(x_i/\gamma), \quad (3)$$

where  $\gamma > 0$  is a smooth parameter. Eq. 3 approximates the maximum value given input  $x_1, \dots, x_n$ .

**Prediction.** The probabilistic logical entailment is computed by the bi-directional message-passing. Let  $\mathbf{x}_{atoms}^{(0)} \in [0, 1]^{|\mathcal{G}|}$  be input node features, which map a fact to a scalar value, RG be the reasoning graph,  $\mathbf{w}$  be the rule weights,  $\mathcal{B}$  be background knowledge, and  $T \in \mathbb{N}$  be the infer step. For fact  $G_i \in \mathcal{G}$ , DeiSAM computes the probability as:

$$p(G_i | \mathbf{x}_{atoms}^{(0)}, \text{RG}, \mathbf{w}, \mathcal{B}, T) = \mathbf{x}_{atoms}^{(T)}[i], \quad (4)$$

where  $\mathbf{x}_{atoms}^{(T)} \in [0, 1]^{|\mathcal{G}|}$  is the node features of atom nodes after  $T$ -steps of the bi-directional message-passing.

## B. DeiVG Datasets

We generated DeiVG dataset using Visual Genome dataset (Krishna et al., 2017). We used the entire Visual Genome dataset to generate deictic prompts and answers out of scene graphs, and we randomly downsampled 10k examples. We only considered the following relations:

- ‘on’
- ‘wearing’
- ‘sitting on’
- ‘wears’
- ‘near’
- ‘made of’
- ‘has’
- ‘along’
- ‘above’
- ‘parked on’
- ‘in front of’
- ‘carrying’
- ‘behind’
- ‘at’
- ‘riding’
- ‘holding’
- ‘under’
- ‘over’
- ‘against’

The prompts are synthetically generated by extracting relations that shares the same subject in the scene. For example, with a pair of VG relations, *“person is holding an umbrella”* and *“person on a boat”*, we generate a deictic prompt, *“an object that is holding an umbrella, and that is on a boat”*. Subsequently, the corresponding answer is extracted from the scene graph. We provide two instances in the generated DeiVG<sub>2</sub> dataset in the following.

```
{
  deictic_prompt: "an object that is on a sofa, and that is on a book",
  answer: [{"name": "paper",
            "h": 32,
            "synsets": ["paper.n.01"],
            "object_id": 2687751,
            "w": 61,
            "y": 236,
            "x": 272}],
  VG_image_id: 2376540,
  VG_data_index: 44297
}
{
  deictic_prompt: "an object that has a shadow, and that is wearing a black shirt",
  answer: [{"h": 50,
            "object_id": 1001275,
            "merged_object_ids": [1001270],
            "synsets": ["man.n.01"],
            "w": 21, "y": 333,
            "x": 47,
            "names": ["man"]}],
  VG_image_id: 2365153,
  VG_data_index: 55196
}
```

### B.1. Additional Analysis on VG Scene Graphs

In Fig. 10, the plot on the left depicts the distribution of the least frequent tail object types on the latest extended version (VG<sub>v1.4</sub>) in comparison to the older version (VG) (Krishna et al., 2017). Object types are sorted with respect to the number of occurrences (x-axis). In the non-frequent range of 0 to 1000, VG<sub>v1.4</sub> contains object types that never appear on the older version (VG), revealing these tail classes of object types are completely missing in the processed older annotations (Xu et al., 2017), which are commonly used for benchmarking SGGs. Moreover, the bar plot on the right indicates a notable increase in the number of object types and total object counts in VG<sub>v1.4</sub> in comparison to VG, making it difficult for SGGs that are pre-trained on the older version to achieve high performance on the DeiVG dataset built upon VG<sub>v1.4</sub>.

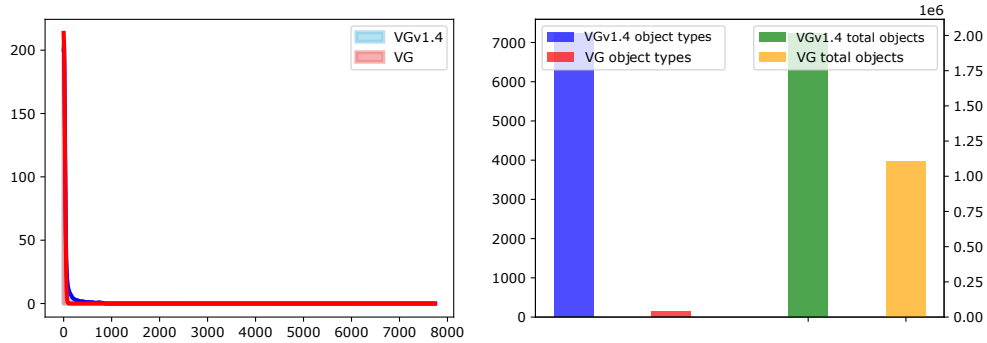


Figure 10. Further comparisons of  $VG_{v1.4}$  with VG. The plot on the left depicts the distribution of the least frequent tail object types of the latest extended version ( $VG_{v1.4}$ ) in comparison to the older version (VG) (Krishna et al., 2017). Object types are sorted w.r.t. the number of occurrences (x-axis). The plot on the right shows the comparison of the number of object types and the number of total objects in the datasets.  $VG_{v1.4}$  contains many more object types than VG, making it difficult for SGGs that are pre-trained on the older version to achieve high performance. (Best viewed in color)

### C. Details of Experiments

We provide details of the models used in the evaluation. For all methods using SAM for segmentation—including DeiSAM—we use the same publicly available SAM checkpoint<sup>6</sup>.

**DeiSAM.** We used NEUMANN (Shindo et al., 2023b) with  $\gamma = 0.01$  for soft-logic operations, and the number of inference steps is set to 2. We set the box threshold to 0.3 and the text threshold to 0.25 for the SAM model. All generated rules are assigned a weight of 1.0. If no targets are detected, DeiSAM produces a mask of a randomly chosen object in the scene.

For LLMs, we provided few-shot examples of deictic prompts and desired outputs in the input context:

Examples:

```
an object that is next to a keyboard.
available predicates: next_to
cond1(X):-next_to(X,Y),type(Y,keyboard).
target(X):-cond1(X).
```

```
an object that is on a desk.
available predicates: on
cond1(X):-on(X,Y),type(Y,desk).
target(X):-cond1(X).
```

```
an object that is on a ground, and that is behind a white line.
available predicates: on,behind
cond1(X):-on(X,Y),type(Y,ground).
cond2(X):-behind(X,Y),type(Y,whiteline).
target(X):-cond1(X),cond2(X)
```

```
an object that is near a desk and against wall.
available predicates: near,against
cond1(X):-near(X,Y),type(Y,desk).
cond2(X):-against(X,Y),type(Y,wall).
target(X):-cond1(X),cond2(X).
```

```
an object that has sides, that is on a pole, and that is above a stop sign.
available predicates: has,on,above
cond1(X):-has(X,Y),type(Y,sides).
cond2(X):-on(X,Y),type(Y,pole).
cond3(X):-above(X,Y),type(Y,stopsign).
target(X):-cond1(X),cond2(X),cond3(X).
```

<sup>6</sup>[https://huggingface.co/spaces/abhishek/StableSAM/blob/main/sam\\_vit\\_h\\_4b8939.pth](https://huggingface.co/spaces/abhishek/StableSAM/blob/main/sam_vit_h_4b8939.pth)

Model	Corr. Predicates (%) ↑			Corr. Rules (%) ↑			Combined (%) ↑		
	DeiVG <sub>1</sub>	DeiVG <sub>2</sub>	DeiVG <sub>3</sub>	DeiVG <sub>1</sub>	DeiVG <sub>2</sub>	DeiVG <sub>3</sub>	DeiVG <sub>1</sub>	DeiVG <sub>2</sub>	DeiVG <sub>3</sub>
Mistral-7B-Instruct	75.50	75.52	67.80	86.95	82.56	75.43	65.88	64.63	51.50
Llama-2-7B-Chat	75.03	26.91	12.47	<b>98.29</b>	96.36	95.22	74.06	25.92	12.06
Llama-2-13B-Chat	92.87	97.19	<b>96.05</b>	97.88	<b>97.82</b>	97.13	91.00	95.17	<b>93.45</b>
GPT-3.5-turbo	<b>96.57</b>	<b>97.43</b>	93.21	97.45	96.96	95.04	<b>95.66</b>	<b>95.36</b>	89.92

Table 4. Performance in logic rule generation of various large language models. We report the success rate of extracting the correct predicates and generating the correct rules in isolation since the predicates are supplied as context for rule generation. The combined success rate are the percentage of samples were both are correct.

```

an object that is wearing a shirt, that has a hair, and that is wearing shoes.
available predicates: wearing,has,wearing
cond1(X):-wearing(X,Y),type(Y,shirt).
cond2(X):-has(X,Y),type(Y,hair).
cond3(X):-wearing(X,Y),type(Y,shoes).
target(X):-cond1(X),cond2(X),cond3(X).
    
```

These few-shot examples improved the quality of the rule generation that follows a certain format.

**GroundedSAM.** We used a publicly available GroundedDino version<sup>7</sup> with Swin-B backbone, pre-trained on COCO, O365, GoldG, Cap4M, OpenImage, ODinW-35 and RefCOCO. We set the box threshold to 0.3 and the text threshold to 0.25 for the SAM model.

**GLIP** We used a publicly available version of GLIP-L<sup>8</sup> with a Swin-L backbone and pre-trained on FourODs, GoldG, CC3M+12M, SBU. We set the prediction threshold to 0.4.

**OFA** We used a publicly available version of OFA-Large<sup>9</sup> fine-tuned for visual grounding.

**SEEM** We used a publicly available checkpoint of SEEM<sup>10</sup> with Focal-L backbone.

**Evaluation Metric.** We used mean average precision (mAP) to evaluate segmentation models. Segmentation masks are converted to corresponding bounding boxes by computing their contours, and then mAP is computed by comparing them with the ground truth bounding boxes provided by Visual Genome.

### C.1. Ablations

Subsequently, we present detailed results corresponding to the ablation studies in Sec. 5.4.

First, we evaluated multiple open and closed-source language models of different sizes on rule generation. The results on correct predicate identification and rule generation are reported in Tab. 4. In general, all instruction-tuned models can generate logical rules from deictic prompts. However, larger models strongly outperform smaller ones, especially for more complex inputs. Interestingly, the types of failure cases differ significantly between models. For example, both Llama models and GPT-3.5-turbo rarely make syntactical errors in rule generation (< 1%), whereas most of Mistral-7B’s incorrect rules are already syntactically unsound.

For the semantic unification task we compare various semantic embedding models as shown in Table 5.

### C.2. Learning to Segment Better

**Dataset.** Let  $(x, p) \in \mathcal{D}$  be a DeiVG dataset, where  $x$  is an input image, and  $p$  is a deictic prompt and  $(o_1, \dots, o_m) \in \mathcal{A}$  be the answers, where  $o_1, \dots, o_m$  are correct target objects to be segmented specified by the prompt. For each input, DeiSAM produces segmentation masks with their confidence:

$$\{(\mathbf{M}_i, s_i)\}_{i=0,\dots,n} = f_{deisam}(x, p), \tag{5}$$

<sup>7</sup> [https://github.com/IDEA-Research/GroundingDINO/releases/download/v0.1.0-alpha2/groundingdino\\_swinb\\_cogcoor.pth](https://github.com/IDEA-Research/GroundingDINO/releases/download/v0.1.0-alpha2/groundingdino_swinb_cogcoor.pth)

<sup>8</sup> [https://huggingface.co/GLIPModel/GLIP/blob/main/glip\\_large\\_model.pth](https://huggingface.co/GLIPModel/GLIP/blob/main/glip_large_model.pth)

<sup>9</sup> [https://modelscope.cn/models/iic/ofa\\_visual-grounding\\_refcoco\\_large\\_en/summary](https://modelscope.cn/models/iic/ofa_visual-grounding_refcoco_large_en/summary)

<sup>10</sup> [https://huggingface.co/xdecoder/SEEM/resolve/main/seem\\_focall\\_v0.pt](https://huggingface.co/xdecoder/SEEM/resolve/main/seem_focall_v0.pt)

Model	Unification Success (%) $\uparrow$
Glove-Wiki-Gigaword	52.27
Word2Vec-Google-News	55.03
OpenAI-CLIP ViT-B/32	52.90
DFN5B-CLIP ViT-H/14	66.65
MonarchMixer-Bert	30.15
MPNet-Base-v2	<b>71.62</b>
MiniLM-L6-v2	62.79
OpenAI-ada-002	66.50

Table 5. Comparison of various embedding models on the semantic unification step in the DeiSAM pipeline. The task is to identify one synonymous object name out of all objects in a scene, given their embedding similarity. Success rate is reported over ca. 2.5k scenes from Visual Genome.

where  $\mathbf{M}_i$  is the  $i$ -th predicted segmentation mask and  $s_i$  is the confidence score. For each mask  $\mathbf{M}_i$ , we consider a binary label  $y_i \in \{0, 1\}$  by computing its corresponding bounding box and using the IoU score, which assesses the quality of bounding boxes:

$$y_i = \begin{cases} 1 & \text{if } \max_j \text{IoU}(\mathbf{B}_i, \mathbf{O}_j) > \theta \\ 0 & \text{otherwise} \end{cases} \quad (6)$$

where  $\theta > 0$  is a threshold,  $\mathbf{B}_i$  is a bounding box computed from mask  $\mathbf{M}_i$ , and  $\mathbf{O}_j$  is a mask that represents answer object  $o_j$ . We extracted instances from DeiVG datasets not used in VETO training (ca. 2000 samples), which are divided into training, validation, and test splits that contain 1200, 400, and 400 instances, respectively. If no targets are detected by the the forward reasoner, DeiSAM produces a mask of a randomly chosen object in the scene, *i.e.*, if the maximum confidence score for targets is less than 0.2, DeiSAM was set to sample a random object in the scene and segment with a confidence score randomly sampled from a uniform distribution with a range of  $[0.1, 0.4]$ .

**Optimization.** We used the RMSProp optimizer with a learning rate of  $1e - 2$ , and performed 200 steps of weight updates with a batch size of 1. The reasoners’s inference step was set to 4. We used IoU score’s threshold was set to  $\theta = 0.8$ .

## D. Additional Segmentation Results

We provide supplementary results of the segmentation on the DeiVG dataset in Fig. 11.

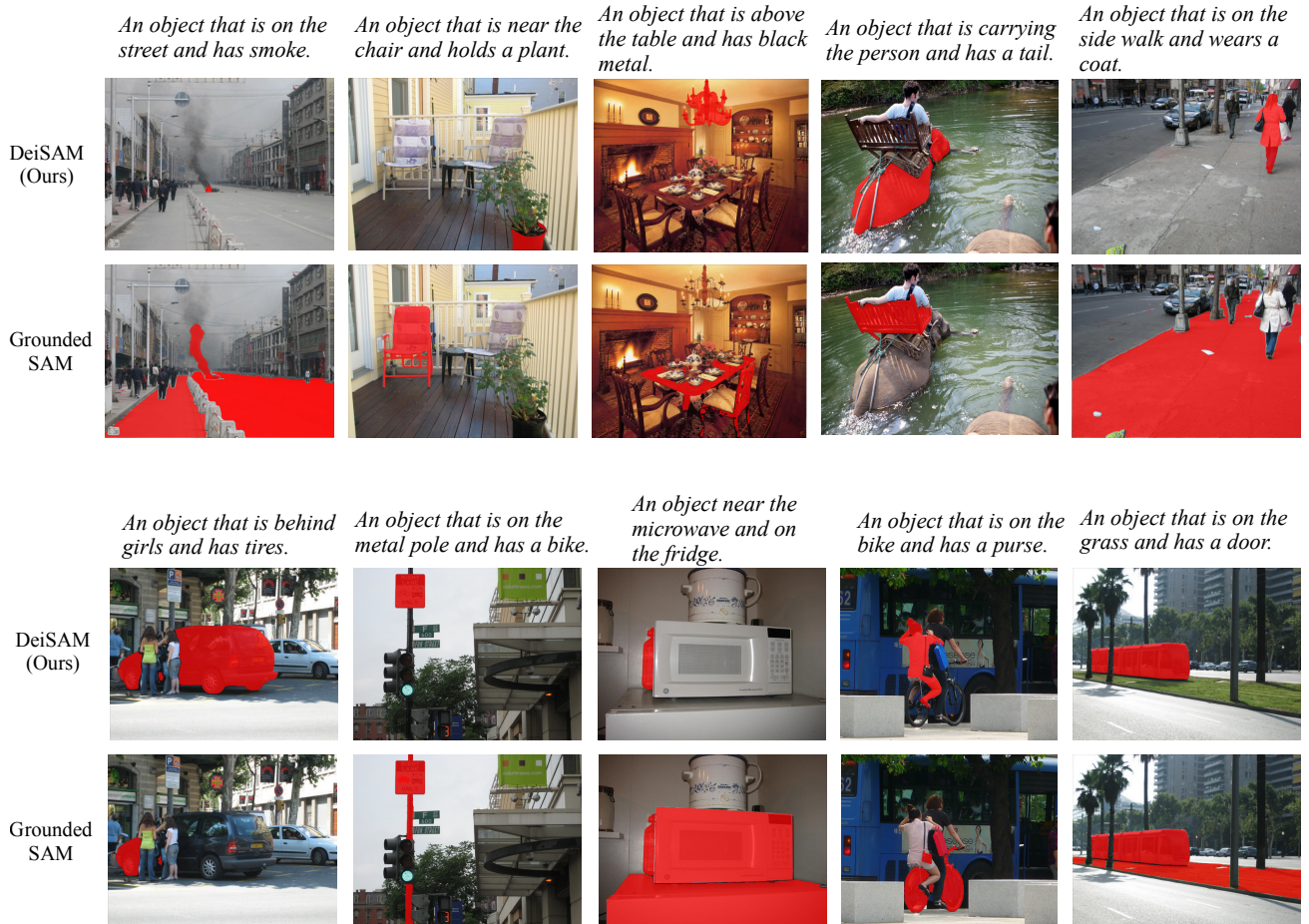


Figure 11. Segmentation results on the DeiVG dataset using DeiSAM and GroundedSAM are shown with deictic prompts.